Grenze International Journal of Engineering and Technology, Jan Issue

Detection of Cancer Cells on Human Thyroid Gland using Bi-static H-Profile Microstrip Antenna with Patch

Nandagopal R[1], Muralidharan D[2], Dr.S.Saranya[3] and Ms.Bindu Babu[4]
[1-4]Easwari Engineering College, Chennai, India
Email: nandagopal304@gmail.com, abhimuraliadhina@gmail.com, nimmycharan@gmail.com and bindu.k@eec.srmrmp.edu.in

***Abstract*— This research paper presents an innovative application of microstrip antenna with patch technology for the detection of cancer cells within the thyroid gland. The Bi-static H-profile microstrip antenna with patch, designed to operate in the microwave frequency range, interacts with the electromagnetic properties of thyroid tissue, allowing for the detection of cancerous cell growth. When the radiator is situated on the human thyroid gland, its performance can exhibit variations. To assess its behaviour, measurements are taken for parameters including return loss, gain, directivity, and e-field pattern. The paper focuses on the development of a bio-compatible and low-profile microstrip antenna with patch system, optimized for efficient electromagnetic coupling with thyroid tissues. This approach addresses the pressing need for cost-effective and non-invasive thyroid cancer screening methods, emphasizing the potential of microstrip antenna with patch in advancing medical diagnostics. The modeling of the thyroid gland and the proposed Bi-static H-profile microstrip antenna with patch is carried out utilizing the CST (Computer Simulation Technology) microwave studio tool.**

***Index Terms*— Bi-Static H-profile MAWP, Return loss, Gain, Directivity, E-Field pattern, Specific Absorption Ratio (SAR)**

I. INTRODUCTION

The thyroid gland, a small butterfly-shaped organ at the base of the neck, is vital for regulating various bodily functions by producing thyroid hormones (T4 and T3). Thyroid cancer, although relatively rare, can have significant health implications, with papillary and follicular thyroid cancers being the most common types. Factors like genetics, radiation exposure, and certain inherited conditions contribute to its development.

Early detection is key for successful treatment, often involving surgery, radioactive iodine therapy, or hormone replacement therapy. Microstrip antennas satisfy various criteria; however, they inherently exhibit limited bandwidth performance. [13]. As medical technology evolves, innovative diagnostic approaches are explored, and microwave imaging techniques emerge as a promising, non-invasive, and radiation-free alternative for assessing thyroid abnormalities. The antenna has the capability to identify cancer by analyzing the distinct material properties within the phantom, which subsequently lead to alterations in the S11 parameter values [5]. Microstrip antennas are valued for their compact design and capability to generate broadside radiation patterns with moderate gains. They have consistently been acknowledged as outstanding conformal radiators. [15]. The Microstrip Reflect Array (MRA) comprises a coaxially fed Microstrip Antenna (MSA) that illuminates a far-field-coupled

Grenze ID: 01.GIJET.10.1.213

array of microstrip patches. [14]. Microwave imaging, utilizing electromagnetic waves, offers detailed internal thyroid gland images, with antennas playing a crucial role in this process. The penetration of microwaves into tissues allows for a more comprehensive assessment, potentially improving diagnostic accuracy. In multi-static microwave imaging (MWI), a sequential transmission approach is employed, with each antenna taking its turn to transmit signals, while the remaining antennas receive the reflected signals [8].

Transitioning from thyroid-related health concerns, this paper introduces a design featuring a Bi-static H-profile microstrip antenna with patch. Renowned for its distinctive features, this antenna finds versatile applications in wireless communication. The H-profile configuration enhances overall performance and functionality, as demonstrated by simulation results obtained using the commercial CST software. FR-4 (with loss-free characteristics) is employed as a substrate to address issues related to low gain and high return loss. The Block Diagram of the Methodology is shown in Fig 1.

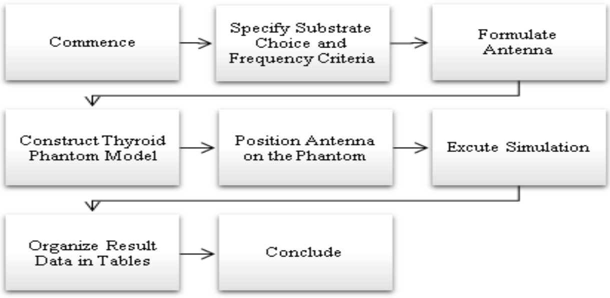

Figure 1. Block Diagram of the Proposed Methodology

II. Literature Survey

The H-profile microstrip antenna with patch, featuring a linear slot and a tumor, achieves a substantial gain of 6.36dB at a frequency of 16.452GHz. SAR values are calculated for 1g of tissue, both with and without the tumor. In the presence of the tumor, the H-profile microstrip antenna with patch with a linear slot yields a notable SAR value of 0.0199W/Kg at a frequency of 10.846GHz [1].

The radar-based MWI works in the frequency domain and involves measuring S11 at different positions on a breast phantom. The MWI process comprises identifying cancerous cell frequencies and using S11 data sets for imaging. A MATLAB-based GUI creates 2D images of the breast phantom, aiding in cancerous cell location prediction and supporting biomedical MWI assessment [2].

A wearable antenna with patch with a Z-shaped design operates within a frequency band of 2.52GHz. The utilization of a substrate with silk results in a decrease in the SAR value. The antenna design yields a gain value of 1.67dB. The presence or absence of thyroid cancer impacts the antenna's performance characteristics [3].

A woven textile with multiple layers and coaxial feeding, intended for wearable applications operating at 2.45GHz, demonstrates diverse Specific Absorption Rate (SAR) values across distinct body regions. In simulations, the SAR value for the arm is calculated to be 0.0164W/Kg. [11].

III. Microstrip Antenna With Patch

A antenna with patch with a microstrip includes of a thin square patch comprising a plane to the ground on one side and a dielectric substrate on the other. The rectangular antenna with patches is the fundamental and common microstrip antenna with patch arrangement. The radiating material Cu (Copper) or Au (Gold) utilized to construct the antenna patch can be structured in any manner such as rectangular, circular, triangular, elliptical, and other popular forms. The rectangular microstrip antenna with patch is shown in Fig 2.

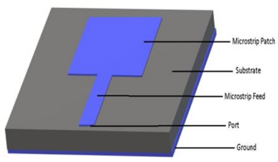

Figure 2. Rectangular MAWP

IV. Design Of The Proposed Antenna

In this study, we employed a H-profile Bi-static microstrip antenna with patch using FR-4 substrate known for its low loss characteristics, featuring a dielectric constant of 4.3. Copper (tempered) is utilized for both the ground and the patch components. The width of the microstrip feed line was determined through careful impedance matching techniques, optimizing the antenna's overall performance.

A. H-profile Microstrip Antenna with patch

The H-profile microstrip antenna with patch incorporates three main parts: a ground, substrate, and patch shown in Fig 3. Thin microstrip line feed is the type of feed applied in this Model, and their width and length are 3.137mm and 20mm, respectively. Generally, the ground and substrate are built with the same length and width, measuring 51.34mm and 59.41mm respectively. The patch width and length are 49.41mm and 41.34mm respectively. Both the substrate and the ground employed in this antenna have a thickness of 1.6 mm and 0.035mm respectively. The slots width and length are 30mm and 20mm respectively.

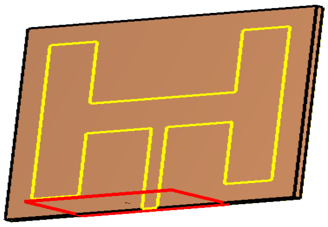

Figure 3. H-profile MAWP

B. Performance of H-profile MAWP in Free Space

Antenna performance in free space is evaluated through key parameters: return loss, Gain, and Directivity. The values are listed in Table I.Simulated results of return loss, gain, and directivity are shown in Fig 4, Fig 5, and Fig 6 respectively.

Table I. Results Of Antenna Performance

Parametres	Results	
	Values	***Units***
Return Loss	-35.59	Db
Gain	7.89	dBi
Directivity	8.62	dBi

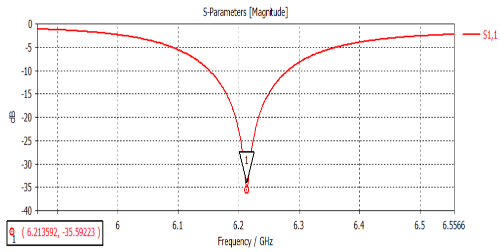

Figure 4. Return Loss of -35.59 at 6.2 GHz Frequency

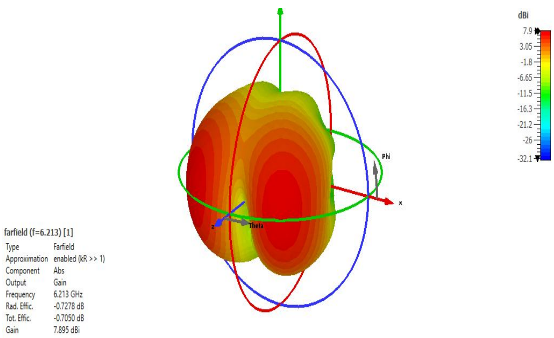

Figure 5. Gain of 7.89 dBi at 6.2 GHz Frequency

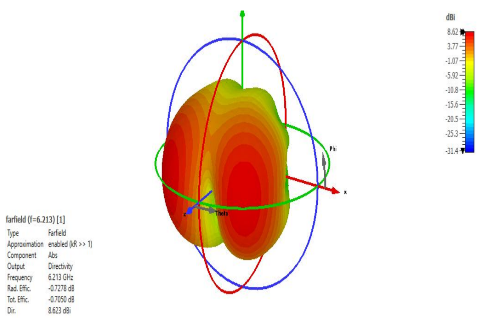

Figure 6. Directivity of 8.62 dBi at 6.2 GHz Frequency

V. Phantom Design

Thyroid cancer affects the minute gland located at the base of the neck, and fortunately, most cases are treatable. When positioning the antenna on the thyroid gland phantom with a tumor, the SAR value is expected to be significantly higher compared to when it is placed on a model without a tumor. The Thyroid phantom model is composed of several distinct components, including skin, fat, bone, the thyroid gland, a tumor, and muscle shown in Fig 7. The suggested phantom model takes the form of a cylindrical structure designed to mimic the human neck area, including the presence of the thyroid gland. The phantom model, in the absence of a tumor, is supplemented with fat and muscle components. The Values are listed in Table II.

TABLE II . VALUES OF THE LAYERS OF THE HUMAN THYROID MODEL

Layers	Values			
	Mass Density ρ (Kg/m^3)	***Permitivity ε (F/m)***	***Conductivity σ (S/m)***	***Thickness (mm)***
Skin	1100	34.94	3.89	1
Fat	950	9.80	0.87	4
Bone	1900	9.58	1.20	9
Thyroid Gland	1050	51.52	5.99	12
Muscle	1140	48.21	5.20	5
Tumour	2160	65.04	9.8	17

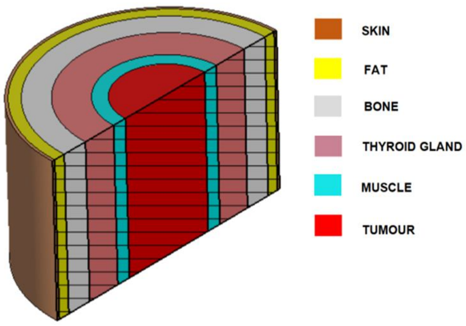

Figure 7. Human Thyroid Gland Model

VI. PLACEMENT OF BI-STATIC H-PROFILE MICROSTRIP ANTENNA WITH PATCH ON PHANTOM MODEL

In our research, we employed a Bi-static H-profile microstrip antenna with patch, and we have detailed its performance in the paper. We conducted a comprehensive analysis of return loss, gain, directivity, and the electric field pattern of both H-profile microstrip antenna with patch (S1, 1 and S2, 2) to differentiate the presence or absence of a tumor. These H-profile antennas were strategically positioned at specific distances from both the positive and negative z-axes of the thyroid gland model to minimize radiation exposure to its maximum extent, ensuring the safety. The Bi-static H-profile microstrip antenna with patch placed on the sides of Phantom with and without tumor are shown in Fig 8 and Fig 9 respectively.

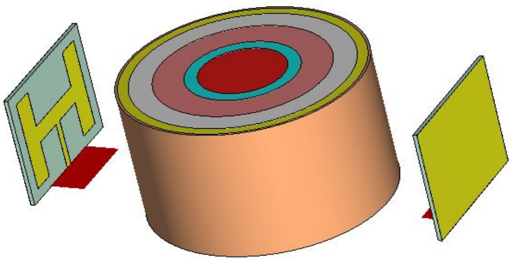
Fig 8. Bi-Static H-profile MAWP on Phantom with Tumour

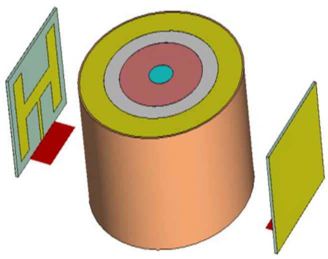
Fig 9. Bi-Static H-profile MAWP on Phantom without Tumour

VII. RESULTS OF BI-STATIC H-PROFILE MAWP ON PHANTOM MODEL

A. Return Loss

The return loss characteristics of the H-profile microstrip antenna with patch are depicted in Fig 10 and Fig 11, showcasing the comparison between antenna performance with and without the presence of a tumor.

For S(1,1), the H-profile MAWP without a tumor exhibits return losses of -22.92 dB at 4.09 GHz, -6.94 dB at 6.4 GHz, and -4.13 dB at 7 GHz. Meanwhile, for S(2,2), the return losses for the same antenna without a tumor are as follows: -15.52 dB at 4.07 GHz, -6.27 dB at 6.36 GHz, and -3.68 dB at 7 GHz.

With the inclusion of a tumor, the H-profile MAWP demonstrates different return loss values at S(1,1): -27.92 dB at 4.11 GHz, -9.79 dB at 6.46 GHz, and -5.60 dB at 7 GHz. For S(2,2), the return losses for the antenna with a tumor are as follows: -24.78 dB at 4.11 GHz, -8.66 dB at 6.45 GHz, and -5.24 dB at 7.1 GHz.

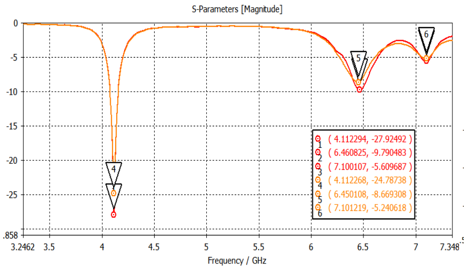

Figure 10. Return Loss of Bi-Static H-profile MAWP placed with Tumour

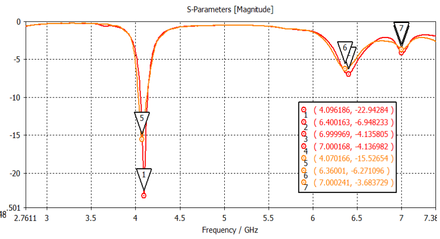

Figure 11. Return Loss of Bi-Static H-profile MAWP placed without Tumour

B. Gain

The Gain characteristics of the H-profile microstrip antenna with patch are depicted from Fig 12 to Fig 15, showcasing the comparison between antenna performance with and without the presence of a tumour.

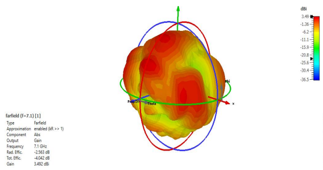

Figure 14. Gain of Bi-Static H-profile MAWP at S(2,2) placed with Tumour at 7.1 GHz

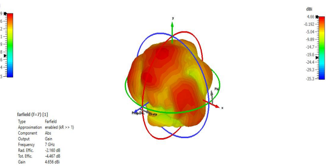

Figure 15. Gain of Bi-Static H-profile MAWP at S(2,2) placed without Tumour at 7 GHz

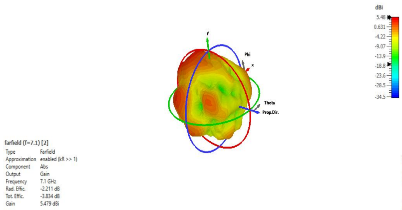

Figure 14. Gain of Bi-Static H-profile MAWP at S(2,2) placed with Tumour at 7.1 GHz

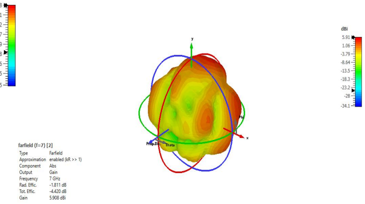

Figure 15. Gain of Bi-Static H-profile MAWP at S(2,2) without Tumour at 7 GHz

C. Directivity

The Directivity characteristics of the H-profile microstrip antenna with patch are depicted from Fig 16 to Fig 19, showcasing the comparison between antenna performance with and without the presence of a tumour.

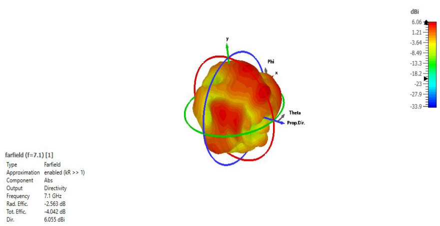

Figure 16. Directivity of Bi-Static H-profile MAWP at S(1,1) placed with Tumour at 7.1 GHz

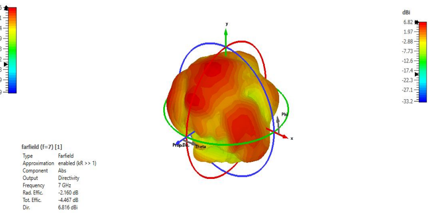

Figure 17. Directivity of Bi-Static H-profile MAWP at S(1,1) placed without Tumour at 7 GHz

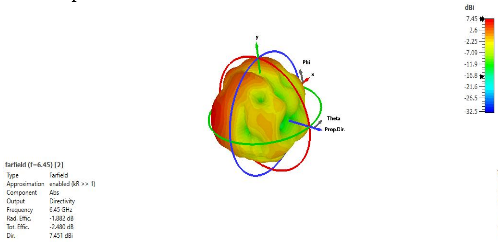

Figure 18. Directivity of Bi-Static H-profile MAWP at S(2,2) placed with Tumour at 6.45 GHz

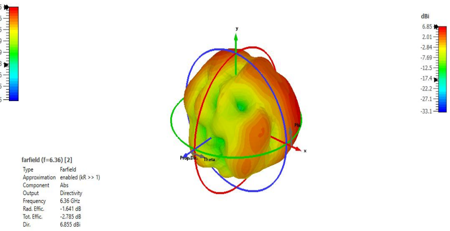

Figure 19. Directivity of Bi-Static H-profile MAWP at S(2,2) placed without Tumour at 6.36 GHz

D. E-field Pattern

The E-field Pattern characteristics of the H-profile microstrip antenna with patch are depicted from Fig 20 to Fig 23, showcasing the comparison between antenna performance with and without the presence of a tumour.

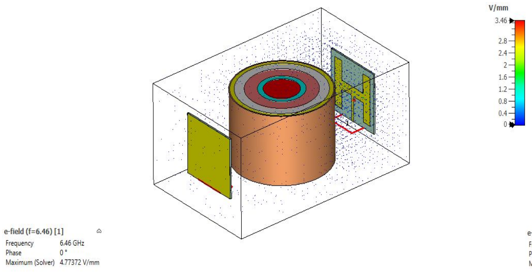

Figure 20. E-field of Bi-Static H-profile MAWP at S(1,1) placed with Tumour at 6.46 GHz

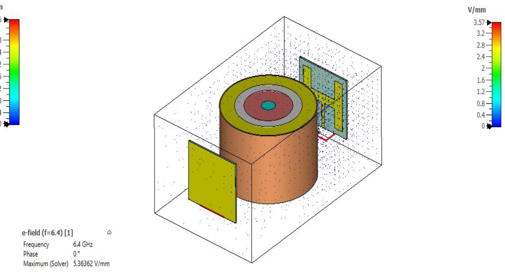

Figure 21. E-field of Bi-Static H-profile MAWP at S(1,1) placed without Tumour at 6.4 GHz

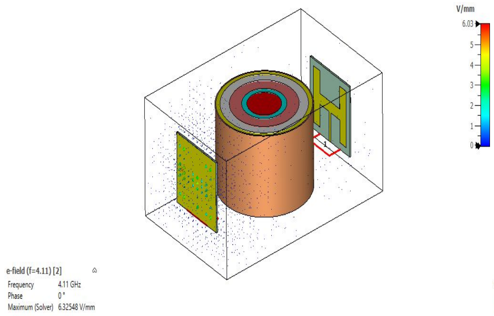

Figure 22. E-field of Bi-Static H-profile MAWP at S (2, 2) placed with Tumour at 4.1 GHz

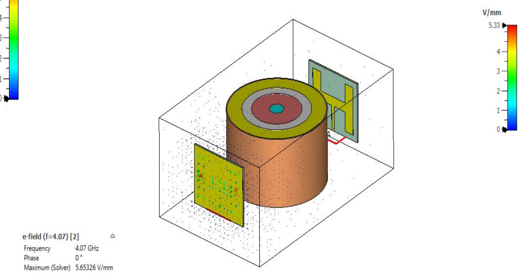

Figure 23. E-field of Bi-Static H-profile MAWP at S (2, 2) placed without Tumour at 4.1 GHz

VIII. Comparison Of The Results Of Bi-Static H-Profile MAWP On Phantom Model

The comparison of S parametres like Return Loss, gain, directivity and E-field Pattern of Bi-static H-profile microstrip antenna with patch placed on with and without tumour cells are tabulated below in Table III, Table IV, Table V and Table VI respectively.

TABLE III. RETURN LOSS WITH AND WITHOUT TUMOUR

Resonant Frequency (GHz)		**Values of Return Loss (dB)**		
With Tumour	***Without Tumour***	***Antenna***	***With Tumour***	***Without Tumour***
4.11	4.09	S(1,1)	-27.92	-22.94
6.46	6.4	S(1,1)	-9.79	-6.94
7.1	7	S(1,1)	-5.60	-4.13
4.11	4.07	S(2,2)	-24.78	-15.52
6.45	6.36	S(2,2)	-8.66	-6.27
7.1	7	S(2,2)	-5.24	-3.68

TABLE IV. GAIN WITH AND WITHOUT TUMOUR

Resonant Frequency (GHz)		**Values of Gain (dBi)**		
With Tumour	***Without Tumour***	***Antenna***	***With Tumour***	***Without Tumour***
4.11	4.09	S(1,1)	-1.7	-2.06
6.46	6.4	S(1,1)	4.79	5.13
7.1	7	S(1,1)	3.49	4.65
4.11	4.07	S(2,2)	-1.45	-2.91
6.45	6.36	S(2,2)	5.56	5.21
7.1	7	S(2,2)	5.49	5.90

IX. Maximum SAR Of The H-Profile MAWP Placed With Tumour

A safe level for the maximum Specific Absorption Ratio(SAR) value of the entire H-profile MAWP when situated within the tumor is 1.01 W/Kg at 4.11 GHz shown in Fig 24.

TABLE V. DIRECTIVITY WITH AND WITHOUT TUMOUR

Resonant Frequency (GHz)		Values of Directivity (dBi)		
With Tumour	***Without Tumour***	***Antenna***	***With Tumour***	***Without Tumour***
4.11	4.09	S(1,1)	3.84	3.75
6.46	6.4	S(1,1)	6.53	6.84
7.1	7	S(1,1)	6.05	6.81
4.11	4.07	S(2,2)	3.69	0.87
6.45	6.36	S(2,2)	7.45	6.85
7.1	7	S(2,2)	7.69	7.71

TABLE VI. E-FIELD PATTERN WITH AND WITHOUT TUMOUR

Resonant Frequency (GHz)		Values of E-field Pattern (V/mm)		
With Tumour	***Without Tumour***	***Antenna***	***With Tumour***	***Without Tumour***
4.11	4.09	S(1,1)	6.44	6.30
6.46	6.4	S(1,1)	4.77	5.36
7.1	7	S(1,1)	5.41	5.59
4.11	4.07	S(2,2)	6.32	5.65
6.45	6.36	S(2,2)	4.93	5.51
7.1	7	S(2,2)	5.48	5.70

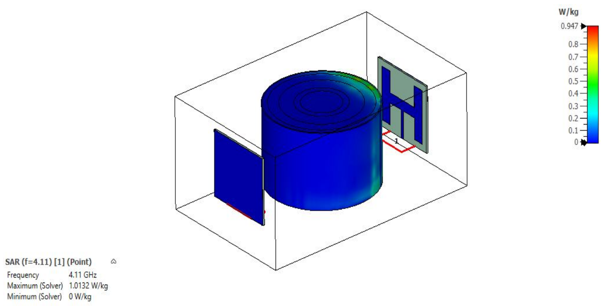

Figure 24. SAR Value of Bi-Static H-profile MAWP at 4.1 GHz

X. CONCLUSION

This research paper presents an innovative Bi-static H-profile microstrip antenna with patch designed for assessing the characteristics of the human thyroid gland model, both with and without tumors, in order to detect the presence or absence of tumor cells. The phantom model is intricately designed with six layers to ensure precise detection. A Bi-Static Antenna is implemented, placed on the sides of the phantom. Notably, at 7 GHz, we observe a significant difference in gain value (1.16 dBi) and directivity value (0.76 dBi). At 4.1 GHz, we notice a substantial variation in the E-field Pattern value (0.65 V/mm).
Moreover, the overall SAR value for the Bi-static H-profile microstrip antenna with patch design, when positioned on the Human Thyroid Gland Model with a tumor, is remarkably low (1.01 W/kg), suggesting its safety for human testing. In the future, it is possible to detect tumor size by comparing changes in antenna performance when different tumor thickness are applied to the phantom model.

REFERENCES

[1] J jenisha and K Madhan kumar, “Design of H-shape Microstrip Antenna with patch for Wearable applications to detect the thyroid gland cancer cells”, ijme,pp. 928-933, 2020
[2] S. Tangwachirapan, P. Sawangsri, P. Pinitkiatisakul, P. Thongdit and W. Thaiwirot, "Breast Cancer Detection Based Microwave Imaging Using Single Antipodal Vivaldi Antenna," 2022 Research, Invention, and Innovation Congress: Innovative Electricals and Electronics (RI2C), Bangkok, Thailand, pp. 97-100,2022
[3] I. Rexiline Sheeba and T. Jayanthy, “Design and Implementation of Flexible Wearable Antenna on Thyroid Gland in the Detection of Cancer Cells”, Biomedical Research, Vol. 29, No. 11, pp. 2307-2312, 2018.
[4] Fengzhow Wang and Tughrul Arslan, “Inkjet-Printed Antenna on Flexible Substrate for Wearable Microwave Imaging Applications”, Proceedings of International Conference on Antennas and Propagation, pp. 1-7, 2016.
[5] Putri Angelia , Wearable Microstrip Antenna with Defected Ground Structure for Breast Cancer Detection , FoITIC, 2020.
[6] C. Rabia, S. Sinan Gultekin, Dilek Uzer, and Ozgur Dundar, “A Microstrip Antenna with patch Design for Breast Cancer Detection,” sci. Direct, 2015.

[7] Yazhou Wang And Mohamed R. Mahfouz “Novel compact tapered microstrip slot antenna for microwave breast imaging” 978-1-4244-9561-0/11/AP-S/URSI 2011.
[8] M. Saraskanroud and I. Jeffrey, “a comparison of time-domain and Frequency-Domain Microwave Imaging of Experimental Targets”, ieee Transactions on computational imaging, vol. 7, pp. 611-623, 2021.
[9] M. Mantash, A.-C. Tarot, S. Collardey, K. Mahdjoubi, "Investigation of Flexible Textile Antennas and AMC Reflectors", International Journal of Antennas and Propagation, vol. 2012, Article ID 236505, 10 pages, 2012
[10] Anzar Khan and Rajesh Nema, “Analysis of Five Different Dielectric Substrates on Microstrip Antenna with patch”, International Journal of Computer Applications, vol. 55, no. 18, pp. 6-12, 2012
[11] E.F. Sundarsingh, M. Kanagasabai and V.S. Ramalingam, “Completely Integrated Multilayered Weave Electro-Textile Antenna for Wearable Applications”, International Journal of Microwave and Wireless Technologies, Vol. 9, No. 10, pp. 2029-2036, 2017.
[12] Min Zhao, Shunlian Chai, Ke Xiao And Xiaotian Zhou “Design of Millimeter-wave Compact Waveguide Slot Coupled Microstrip Array” 978-1-5386-6396-7/18/2018 IEEE.
[13] S.Adnan, R.A.Abd-Alhameed, H.I.Hraga, I.T.E.Elfergani and M.B.Child “CoMAWPct Microstrip Antenna Design for Microwave Imaging” 978-1-4244-7306-9/10/ 9 November 2010.
[14] Amit A. Deshmukh1, Kshitij Lele1, Ami A. Desai1, Saleha A. Shaikh1, Sudesh Agrawal “Broadband E-Shaped Microstrip Reflectarray Antenna with Microstrip Antenna Feed”. 78-1-4673-6981-7/15/ 2015 IEEE.
[15] Qi Wu, Ronghong Jin, and Junping Geng “A Single-Layer Ultrawideband Microstrip Antenna” 0018-926X/2009 IEEE.